POLITECNICO DI TORINO
Repository ISTITUZIONALE

Stress distribution and failure analysis comparison between Zirconia and Titanium dental implants

(Article begins on next page)

01 September 2025

2nd Mediterranean Conference on Fracture and Structural Integrity

Stress distribution and failure analysis comparison between Zirconia and Titanium dental implants

Dario Milone[a], Luca Fiorillo[b], Fabio Alberti[a], Gabriele Cervino[b], Vincenzo Filardi[c], Alessandro Pistone[a], Marco Cicciù[b] and Giacomo Risitano[a]*

[a]*University of Messina, Department of Engineering, Contrada di Dio (S. Agata), 98166 Messina, Italy*

[b] *Department of Biomedical and Dental Sciences, Morphological and Functional Images, University of Messina, Azienda Ospedaliera*

Universitaria "G. Martino", Via Consolare Valeria, 98100 Messina, Italy

[c]*D.A. Research and Internationalization, University of Messina, Via Consolato del mare 41, 98121, Messina, Italy*

Abstract

Orthodontic Titanium implants are the most employed and well investigated in literature. In fact, thanks to its mechanical properties and biocompatibility with the human bone, this material represents one of the best solutions to improve the osseointegration process and implant life. In recent years, the attention was shifted to soft tissue integration which has led to a new solution in terms of implant design and material. According to recent researches, metal-free implants, like Zirconia implant, can improve the biological width and accelerate the osseointegration process. Beyond the advantage in biological terms, the use of Zirconia leads to a different mechanical behaviour concerning Titanium, in particular on the cortical bone.

In this work, the effect that the material change have on the stress distribution around the cortical bone has been analyzed through a Finite Element Analysis (FEA). According to literature of recent years, dental prosthesis of this study has been tested using a compression load applied to the post surface with three different inclinations. The simulation results show that the stress evaluated for Zirconia implant are more distributed around the cortical bone while the stress evaluated for the Titanium implant is extended more over the whole implant. These results confirm that the use of Zirconia could improve the osseointegration process and guarantee a longer life of the implant.

* Corresponding author. Tel.: 389 70 251527
  E-mail address: giacomo.risitano@unime.it

1. Introduction

Since the early dentistry practice, the major request from people has been to restore the chewing function and replace missing teeth. Early dentistry techniques were rudimental and often resulted in a deterioration of the dental implant and diminishing of chewing ability [1]. With scientific progress, has been possible to design dental implant able to accelerate the osseointegration process and improve the quality of life of the patients [2–4]. In the early days, there was a strong focus on osseointegration progress to make sure that the implants have high mechanical strength and on the other hand allows staying in the bone for a long time. In this way, thanks to its mechanical properties and biocompatibility with the human bones, Titanium is largely employed in orthodontic prostheses and is well investigated in literature documentation [5]. In more recent years, the attention is shifted to soft tissue integration. This leads to an increase in the complexity of the solution in terms of both design technique and both material employment, such as composite [6] or 3D biomedical metal materials printed through Additive Manufacturing techniques [7–9]. Stable soft and hard tissue levels are very important for successful long-term results and the composition of the biological width (BW), in terms of connective tissue and epithelium, have a big impact on this. Therefore, a higher proportion of connective tissue gives better protection to the bone-implant interface. Keeping this in mind, a metal-free implant, like Zirconia [10–15], can improve the BW and therefore accelerate osseointegration process. According to Lee et al [16], the proportion of the connective tissue of the total BW for natural teeth (65.8%) is very similar to Zirconia (65.4 %) (metal free material) while Titanium shows a lower proportion (38.1 %). Moreover, the implant design has an important impact on soft and hard tissue integration. Bone level system with micro-gaps and joints deep in the tissues (i.e. with offset and no offset concerning cortical bone) could potentially have an adverse effect on osseointegration process and on mechanical stress distribution [17].

In this work, in order to investigate the effect of prosthesis design and material on mechanical strength, two different types of orthodontic implants have been analysed: full Titanium implant and the implant with integrated abutment made of Zirconia (Z_rO_2) and high tech glass-fibre post. The main goal is to perform a Finite Element Analysis (FEA) [17,18] of both implants and highlight the difference between the two implants, in terms of stress-strain distribution and, if it occurs, failure. The prosthodontic prosthesis in exam presents, in both materials type, an offset of 3mm within the cortical bone. The modelling phase of the dental implant was performed using SpaceClaim® 2022 CAD software, which allows obtaining a detailed 3D model of the implants. Then, a FE analysis was performed using Ansys Workbench 2022R1® software. The FE analysis has been divided into the following two phases: the finite element model construction phase and the post-processing of the results. In the first one, the constrain and load conditions were considered. In particular, three different types of the normalized load were considered: axial vertical load along the z-axis, 15-degree inclination and 30-degree inclination for both materials. This is made to emulate physiological conditions in the oral cavity [19]. Then, both implants have been compared in terms of stress-strain distribution in order to establish which material type is more suitable for this application.

Nomenclature	
E	Isotropic elastic modulus
E_{xx}	Orthotropic elastic modulus along x direction
E_{yy}	Orthotropic elastic modulus along y direction
E_{zz}	Orthotropic elastic modulus along z direction
G	Isotropic shear modulus
G_{xx}	Orthotropic shear modulus along x direction
G_{yy}	Orthotropic shear modulus along y direction
G_{zz}	Orthotropic shear modulus along z direction

ν	Isotropic Poisson's ratio	
ν_{xx}	Orthotropic Poisson's ratio along x direction	
ν_{yy}	Orthotropic Poisson's ratio along y direction	
ν_{zz}	Orthotropic Poisson's ratio along z direction	
ρ	Density	
σ_y	Yield stress	
σ_u	Tensile strength	

2. Materials and methods

The numerical analysis has been carried out on a single tooth orthodontic implant (Figure 1a and 1b). with offset configuration i.e. the conical part of the implant is 3 mm above the cortical bone.
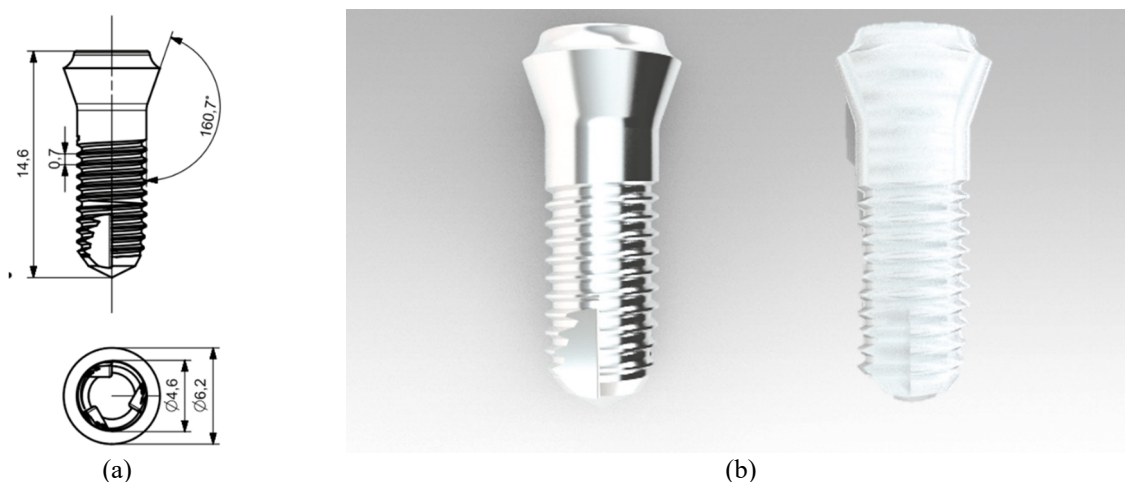

<div align="center">(a)   (b)</div>

Figure 1 Single tooth orthodontic implant a) Prospective view of the implant (all the dimensions are in mm) b) Left side: Titanium implant. Right side: Zirconia implant

The 3D model of the implants has been developed using SpaceClaim® 2021 CAD (Figure 2a) software and the FEA was performed with Ansys Workbench 2021R2® software. Considering that both materials works in the elastic-linear range, the simulation type used is, in this case, linear static structural simulation [20] and it is aimed at investigating the stress-strain distribution of bone, dental implant and post under certain constrain and load conditions. The mesh used for the geometry (Figure 2b) consist of tetrahedral elements with a lower limit of 0.5 mm in size for the implant and 0.3 mm for the bone [20]. Different process regard the post in which SOLID186 elements has been generated, with a minimum size of 0.6 mm. It is a higher order 3-D 20-node solid element that exhibits quadratic displacement behaviour. The element is defined by 20 nodes having three degrees of freedom per node: translations in the nodal x, y, and z directions. The bone mesh has been generated through the "Automatic method" implemented in Ansys. This meshing type allows using of tetrahedral elements to follow as much as possible the surface irregularity and refine the mesh in the areas of interest. The post's mesh has been generated through "MultiZone method" also in this case implemented in Ansys. It allows using hexahedral elements in order to have a smoother mesh on which to apply the load conditions. In both cases, a convergence analysis has been performed in order to choose the optimal mesh size capable of providing accurate results without too long simulation time (Figure 3).
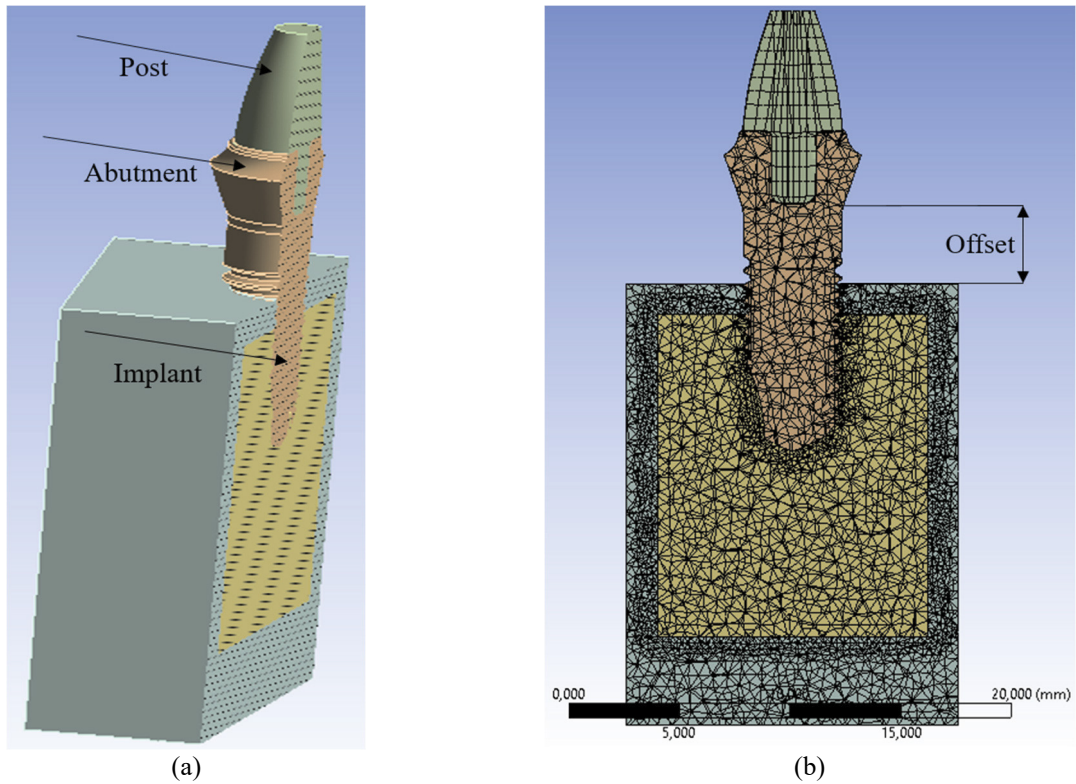
(a)　　　(b)

Figure 2 Single tooth prosthodontic implant. It consists of three main parts: post, abutment and implant. In this configuration is present an offset of 3 mm between the conical part and the cortical bone. a) 3D CAD model b) FE model
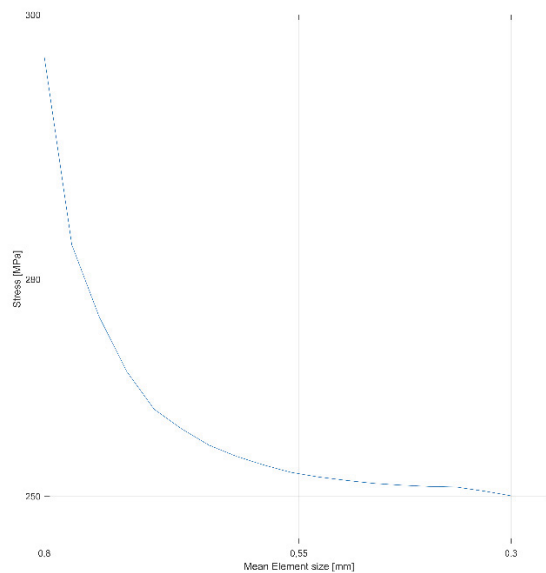

Figure 3 Convergence analysis for the mesh size

Two different materials have been compared: Zirconia (Z_rO_2) and biomedical Titanium (Ti6Al4V). In particular, the first one is completely metal-free and consists in the implant with integrated Zirconia abutment, and post, consist in high-tech glass fibre. The osseous portion has been threaded with a sintering process, resulting 4-5 times rougher than other commercially available implants [21]. Hence, thanks to this process, the osseous surface is homogeneous, hydrophilic and osteoconductive, promoting the osseointegration process. On the other hand, the transgingival part of the implant has a machined surface that promotes soft tissue attachment. According to literature, the Zirconia and the fibre-glass under examination could be considered as homogeneous and isotropic material, while the bone tissues (cortical and cancellous), that should be anisotropic, were considered as orthotropic in the simulation. The material properties of cortical bone, cancellous bone, Zirconia and fibre-glass are reported in Table 1 (according to [22]).

Properties	Cortical Bone	Cancellous Bone	Zirconia (Z_rO_2)	Fibre-Glass
ρ [g/cm³]	1.8	1.2		
E_{xx} [GPa]	9.6	0.144		
E_{yy} [GPa]	9.6	0.099	205	20
E_{zz} [GPa]	17.8	0.344		
v_{xx}	0.55	0.23		
v_{yy}	0.30	0.11	0.3	0.22
v_{zz}	0.30	0.13		
G_{xx} [GPa]	3.10	0.053		
G_{yy} [GPa]	3.51	0.063	78.846	8.1967
G_{zz} [GPa]	3.51	0.045		

Table 1 Material properties of cortical bone, cancellous bone, Zirconia and Fibre-glass [22]

In Table 2 are shown the material properties of Ti6Al4V (according to [23]):

Properties	Value
ρ [g/cm³]	4.4
E [Gpa]	113
G [Gpa]	45
v	0.35
σ_y [Mpa]	786
σ_u [Mpa]	850

Table 1 Material properties of Ti6Al4V [23]

After the definition of implant geometry, mesh and material properties for both cases, constrain and load conditions have been implemented in the model. Fixed support has been used for the front and rear sides of the bone, considering

the continuity of the maxillary bone (Figure 4a). The load condition regard the post surface (Figure 4b) and the implant has been test with a compression load of 400 N. In particular, three different cases have been investigated: pure vertical load along Z-axis, 15-degree inclination and 30-degree inclination. The bone-implant contact condition was modelled as a "frictional" contact system, in order to simulate the osseointegration process of the implant, with a friction coefficient of 0.15[24]. Considering that the post is cemented over the implant, the contact between the post and the implant has been set to "bonded". The same contact condition has been applied to the contact between the cortical bone and the cancellous bone.
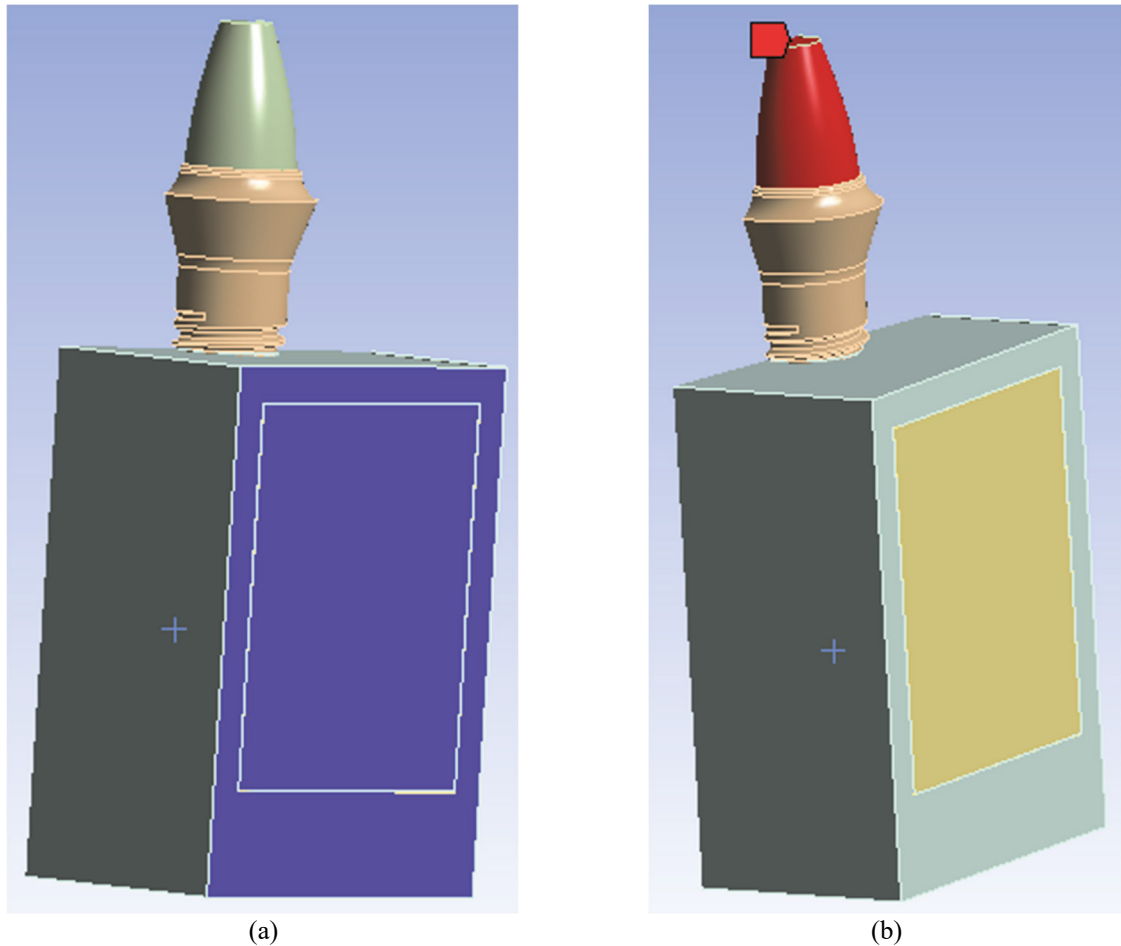

(a)   (b)

Figure 4 Boundary conditions implemented to the FE model (a) Fixed support applied to the front and rear side of the bone (b) Load condition applied to post surface

3. Result and discussions

The stress distribution around the implant has been evaluated and compared for both materials. The result is the analysis of three-dimensional models that consider the risk factors related to bone quality and inflammation. Finite Element Method (FEM) and Finite Element Analysis (FEA) have been extensively applied to simulate the effects of loading on the implant and surrounding bone. As is well known, a finite element model needs to be calibrated based

on experimental tests, to obtain reliable results on material's behaviour. Despite, in this work, there is no experimental characterization of both materials (or the implant itself), a comparison between the two materials subjected to the same load and constrain condition could be very useful. Moreover, the materials properties implemented in the simulations come from scientific study well established. Hence, this study aims to verify the stress on the bone at different load inclinations, and with different materials configurations. For the results obtained, the colour scales have been unified to represent the range of actions on the system. Figure 5 shows the state of stress acting on the whole system during the six tests. To illustrate the stress, a section perpendicular to the two planes in which the constraint was placed was analyzed.
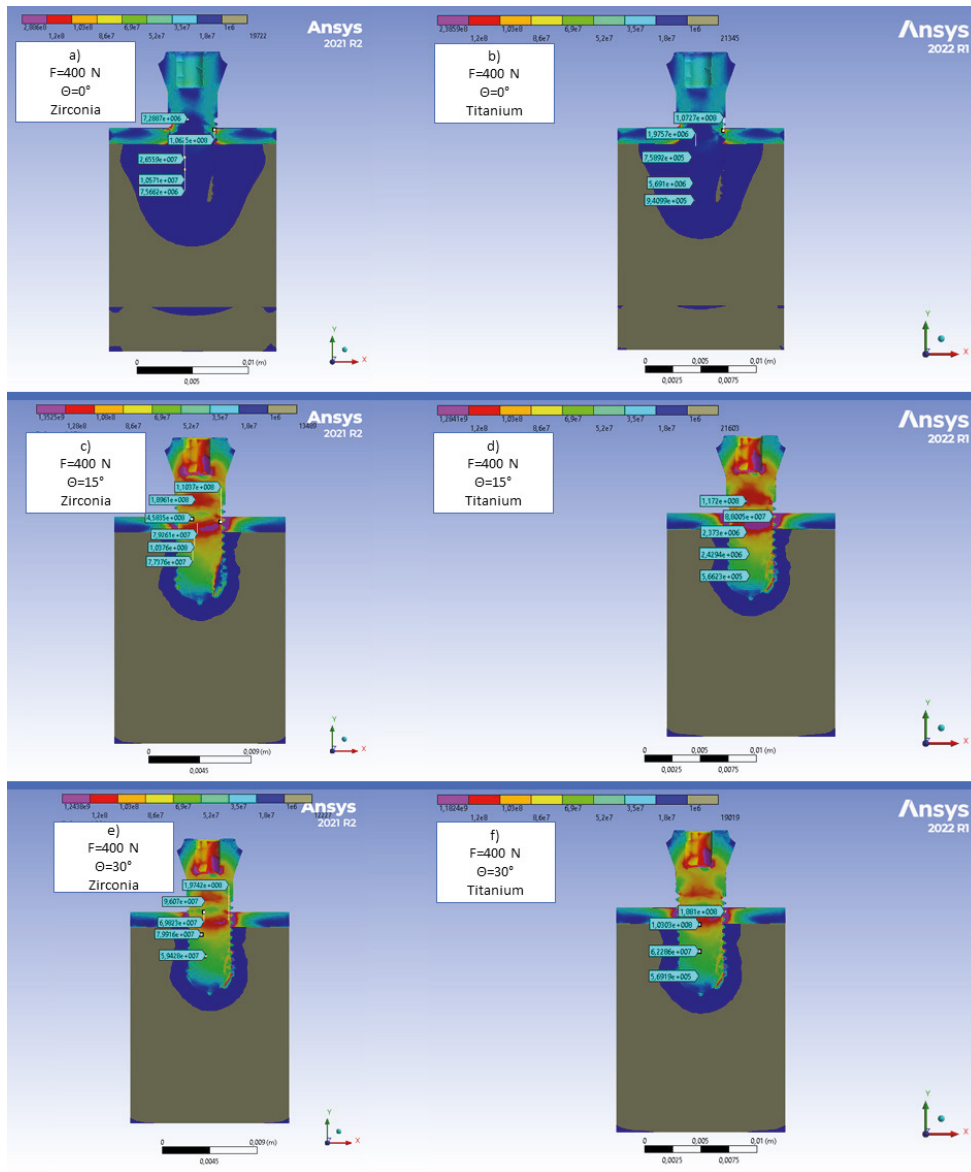

Figure 5 Stress distribution: a) Test I b) Test II c) Test III a) Test IV b) Test V c) Test VI.

From the analysis of Figure 5, it appears that the implant is loaded with a stress that is significantly below its yield

strength. Figure 6, on the other hand, shows that the stress values, especially in the cortical bone region, are close to the yield strength, when the load is parallel to implant axes, while this value is exceeded this range when load increase is an inclination with this axes from parallel direction to 30° direction. Therefore, the load inclination will lead to an instability of the cortical bone causing it to fracture.
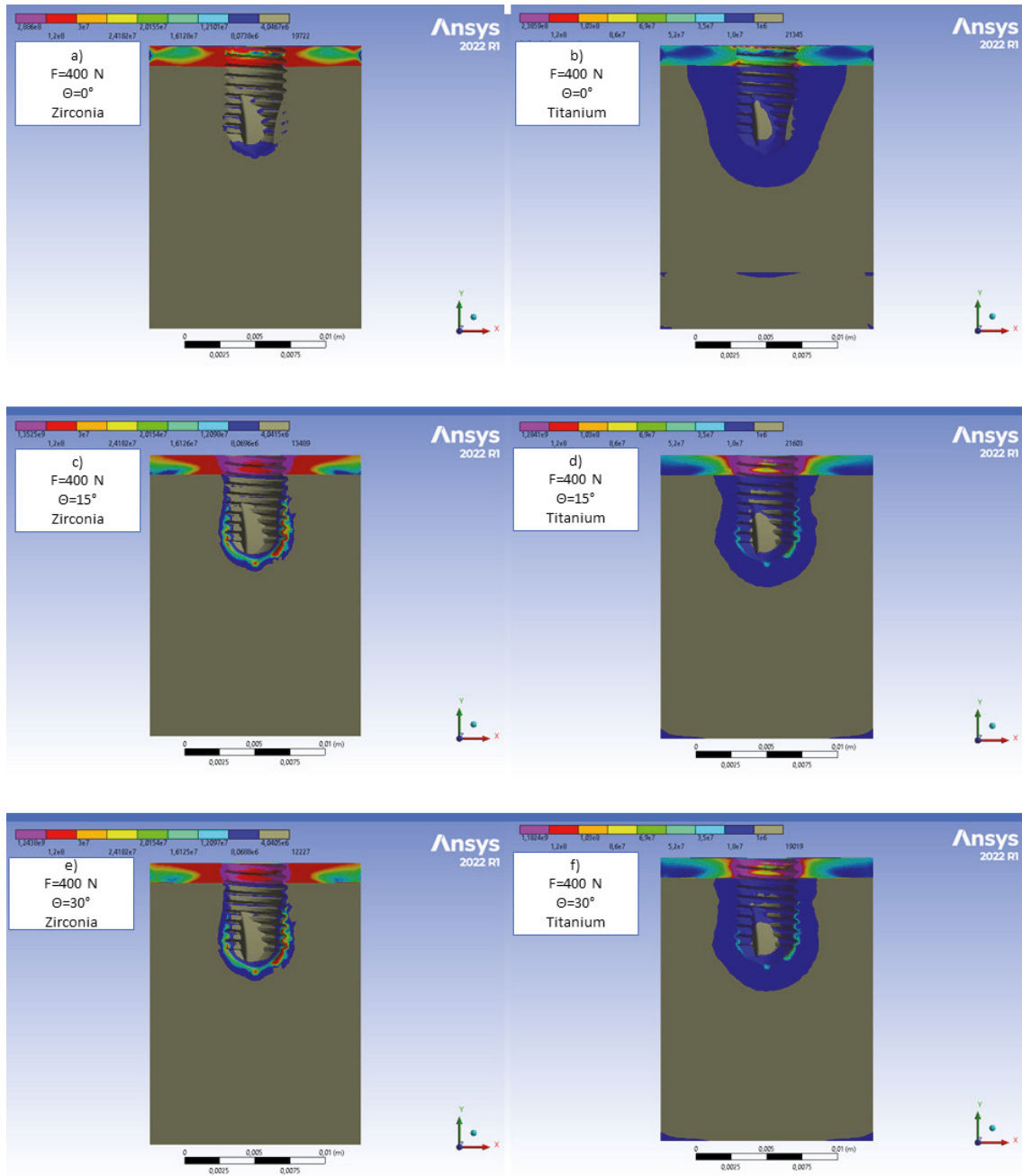

Figure 6 Stress distribution of the cortical bone in the isometric view: a) Test I b) Test II c) Test III a) Test IV b) Test V c) Test VI.

To gain a more detailed insight into the behaviour of the bone, two paths in vertical and horizontal directions were

created, in order to read the stresses along the depth of the bone at the interface with the implant threads and the stresses generated on the cortex as the distance to the prosthesis varied.

From Figure 7, the stress calculated on the bone in the horizontal direction shows a decreasing trend at half the thickness of the cortical bone, starting from a value of 45 MPa (about 40% of the yield). A decreasing trend is also observed for the vertical course. The first value is not considered because the theory underlying the FEA discards the values found at the boundary of a body. Furthermore, it is possible to observe that the peak stress values are very similar for both materials in vertical and horizontal directions. The main difference regards the stress distribution, that tends to decrease more rapidly in Zirconia implant with respect to Titanium implant.
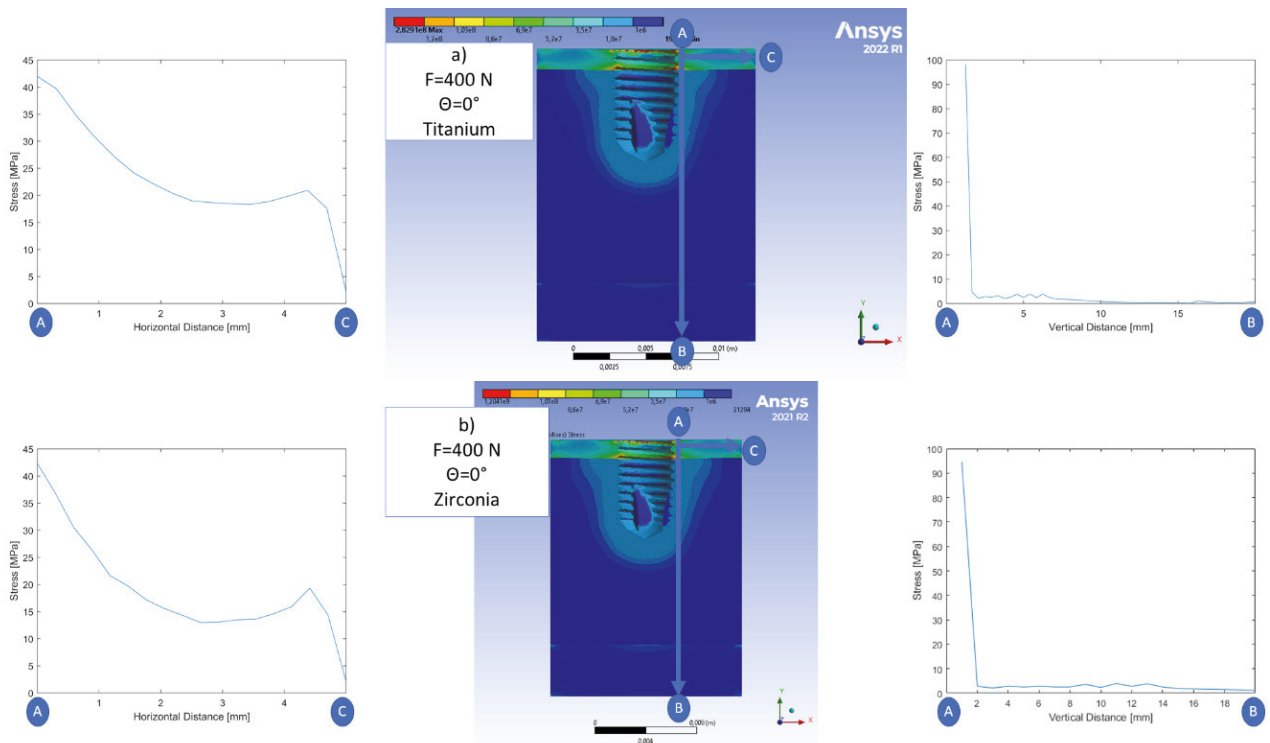

Figure 7 Horizontal and Vertical stress path: a) Test I b) Test II.

Figure 8 shows that the stress calculated on the bone in the horizontal direction has a decreasing tendency, but the calculated value is higher than the yield stress of the bone, indicating a critical condition. A decreasing trend is also seen in the vertical direction. Also in this case, the value of the yield stress of the cortical bone is exceeded, and in this condition the cancellous bone also reaches a state of instability. Another information that can be noticed is that the stress trend is the same from two type of implants. However, it can be seen that in case of using zirconia implant, stress are more distributed around the bone in contrast with titanium implant. This statement is visible by analyzing
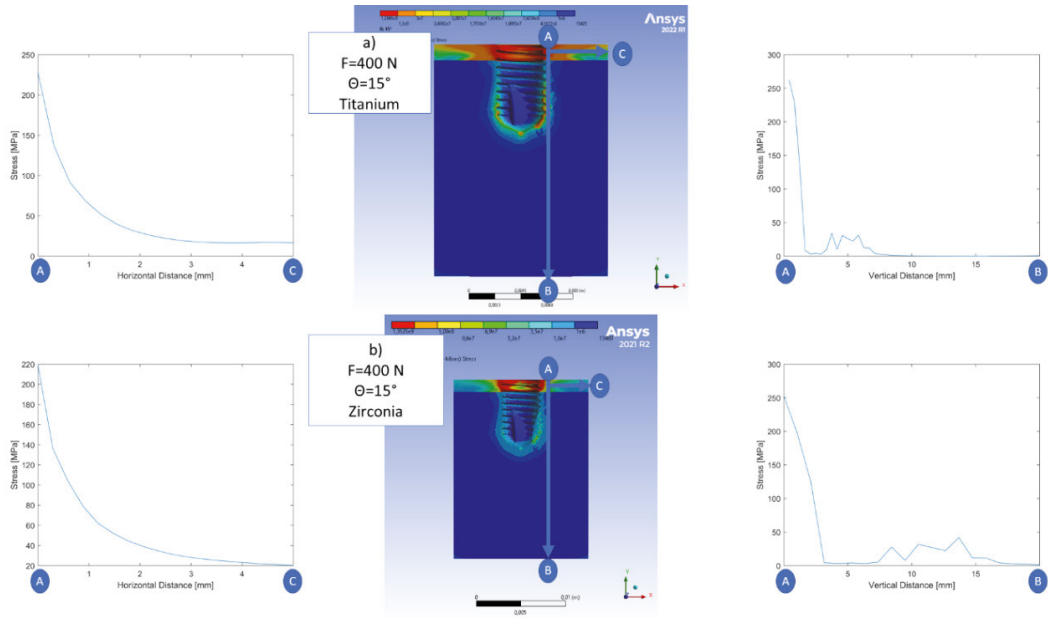
the vertical path graph for both configuration.

Figure 8 Horizontal and Vertical stress path: a) Test III b) Test IV.

From figure 9, the stress calculated on the bones has a decreasing tendency in the horizontal and vertical directions, also in this case the stress on the bones exceeds the yield point. Unlike the previous case, in this case, the average bone stress is higher because the stresses are distributed over a larger part of the bone, but the point values are lower than in the previous case. This could be due to the inclination of the load, which acts on a larger area and increases the stressed area. Also in this case the statements described for the previous test are valid.
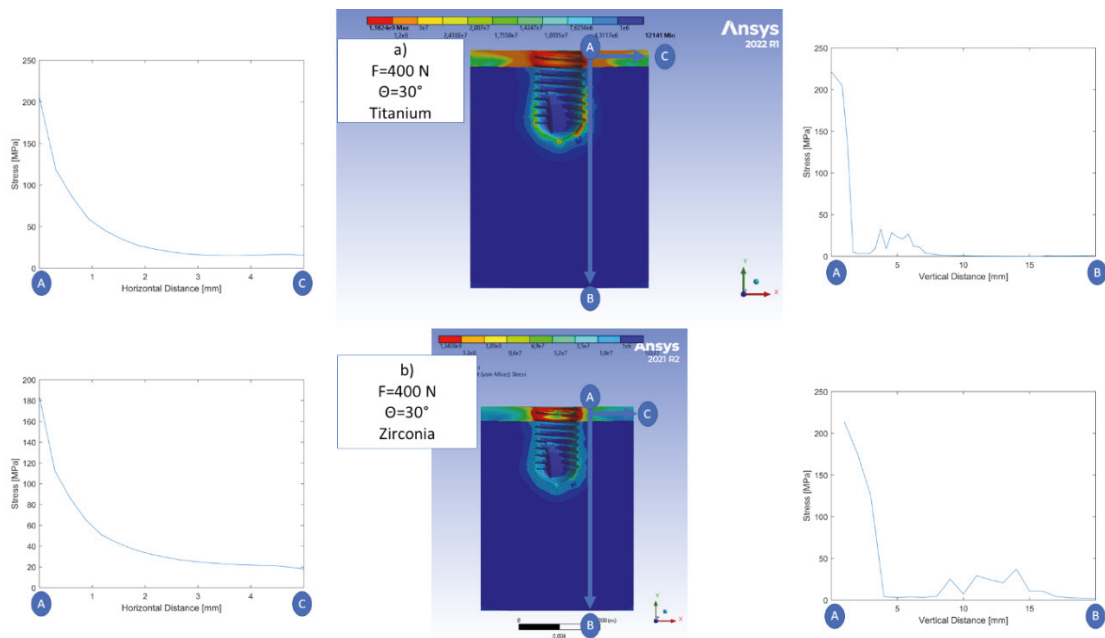

Figure 9 Horizontal and Vertical stress path: a) Test V b) Test VI.

4. Conclusions

In this work, the authors investigated and compared the stress distribution in Zirconia and Titanium dental implants respectively. A compression load of 400 N has been applied to the post surface with three different inclinations:

- 0-degree inclination;
- 15-degree inclination;
- 30-degree inclination.

Analyzing the results is possible to extract the following conclusions:

- The FEA results show that, when the load were applied parallel to the implants axis, the stress values are close to the yield strength, especially in the cortical bone region. However, in this case, the stress values did not lead to the implant failure. In the other cases, on the contrary, the stress values are out of the yield strength, causing an instability of the cortical bone and the implant failure;
- The stress calculated on the bone, both in the horizontal and vertical direction, shows a decreasing trend at half thickness of the cortical bone. Comparing Zirconia implant and Titanium implant stress distribution, is possible to observe that peak values for these two directions are similar, but in zirconia implant, the stress trend decreases faster than in titanium implant;
- It can be seen that in the case of using a zirconia implant, stress is more distributed around the bone in contrast with the titanium implant.

In conclusion, is possible to assert that, despite the better mechanical properties of Titanium, Zirconia material is the best solution for this type of application, where is present an offset between the abutment and the cortical bone. The literature review and the simulation results confirm that the use of a metal-free material like Zirconia leads to an improvement of the osseointegration process and a longer life of the implant.

References

[1] T. Flügge, W.J. van der Meer, B.G. Gonzalez, K. Vach, D. Wismeijer, P. Wang, The accuracy of different dental impression techniques for implant-supported dental prostheses: A systematic review and meta-analysis, Clin. Oral Implants Res. 29 (2018) 374–392. https://doi.org/10.1111/clr.13273.

[2] X. Hao, H. Zhou, B. Mu, L. Chen, Q. Guo, X. Yi, L. Sun, Q. Wang, R. Ou, Effects of fiber geometry and orientation distribution on the anisotropy of mechanical properties, creep behavior, and thermal expansion of natural fiber/HDPE composites, Compos. Part B Eng. 185 (2020) 107778. https://doi.org/10.1016/j.compositesb.2020.107778.

[3] G.R.M. Matos, Surface Roughness of Dental Implant and Osseointegration, J. Maxillofac. Oral Surg. 20 (2021). https://doi.org/10.1007/s12663-020-01437-5.

[4] C.S. Chen, J.H. Chang, V. Srimaneepong, J.Y. Wen, O.H. Tung, C.H. Yang, H.C. Lin, T.H. Lee, Y. Han, H.H. Huang, Improving the in vitro cell differentiation and in vivo osseointegration of titanium dental implant through oxygen plasma immersion ion implantation treatment, Surf. Coatings Technol. 399 (2020) 126125. https://doi.org/10.1016/j.surfcoat.2020.126125.

[5] A. Kurup, P. Dhatrak, N. Khasnis, Surface modification techniques of titanium and titanium alloys for biomedical dental applications: A review, Mater. Today Proc. 39 (2020) 84–90. https://doi.org/10.1016/j.matpr.2020.06.163.

[6] D. D'Andrea, A. Pistone, G. Risitano, D. Santonocito, L. Scappaticci, F. Alberti, Tribological characterization of a hip prosthesis in Si3N4-TiN ceramic composite made with Electrical Discharge Machining (EDM), Procedia Struct. Integr. 33 (2021) 469–481. https://doi.org/10.1016/j.prostr.2021.10.054.

[7] G. Epasto, G. Palomba, D.D. Andrea, S. Di Bella, R. Mineo, E. Guglielmino, F. Traina, Experimental investigation of rhombic dodecahedron micro-lattice structures manufactured by Electron Beam Melting, Mater. Today Proc. 7 (2019) 578–585. https://doi.org/10.1016/j.matpr.2018.12.011.

[8] G. Epasto, G. Palomba, D. D'Andrea, E. Guglielmino, S. Di Bella, F. Traina, Ti-6Al-4V ELI microlattice structures manufactured by electron beam melting: Effect of unit cell dimensions and morphology on mechanical behaviour, Mater. Sci. Eng. A. 753 (2019) 31–41.

https://doi.org/10.1016/j.msea.2019.03.014.

[9] F. Cucinotta, E. Guglielmino, G. Longo, G. Risitano, D. Santonocito, F. Sfravara, Topology optimization additive manufacturing-oriented for a biomedical application, Springer International Publishing, 2019. https://doi.org/10.1007/978-3-030-12346-8_18.

[10] A. Winkelhoff, M. Cune, Zirconia Dental Implants: A Clinical, Radiographic, and Microbiologic Evaluation up to 3 Years, Int. J. Oral Maxillofac. Implants. 29 (2014) 914–920. https://doi.org/10.11607/jomi.3293.

[11] J. Becker, G. John, K. Becker, S. Mainusch, G. Diedrichs, F. Schwarz, Clinical performance of two-piece zirconia implants in the posterior mandible and maxilla: a prospective cohort study over 2 years, Clin. Oral Implants Res. 28 (2017) 29–35. https://doi.org/10.1111/clr.12610.

[12] D.S. Thoma, I. Sailer, S. Mühlemann, A. Gil, R.E. Jung, C.H.F. Hämmerle, Randomized controlled clinical study of veneered zirconia abutments for single implant crowns: Clinical, histological, and microbiological outcomes, Clin. Implant Dent. Relat. Res. 20 (2018) 988–996. https://doi.org/10.1111/cid.12674.

[13] T. Hanawa, Zirconia versus titanium in dentistry: A review, Dent. Mater. J. 39 (2020) 24–36. https://doi.org/10.4012/dmj.2019-172.

[14] S. Roehling, M. Astasov-Frauenhoffer, I. Hauser-Gerspach, O. Braissant, H. Woelfler, T. Waltimo, H. Kniha, M. Gahlert, In Vitro Biofilm Formation on Titanium and Zirconia Implant Surfaces, J. Periodontol. 88 (2017) 298–307. https://doi.org/10.1902/jop.2016.160245.

[15] B. Derbyshire, J. Fisher, D. Dowson, C. Hardaker, K. Brummitt, Comparative study of the wear of UHMWPE with zirconia ceramic and stainless steel femoral heads in artificial hip joints, Med. Eng. Phys. 16 (1994) 229–236.

[16] D.J. Lee, J.S. Ryu, M. Shimono, K.W. Lee, J.M. Lee, H.S. Jung, Differential healing patterns of mucosal seal on zirconia and titanium implant, Front. Physiol. 10 (2019) 1–11. https://doi.org/10.3389/fphys.2019.00796.

[17] M. Cicciù, G. Cervino, D. Milone, G. Risitano, FEM analysis of dental implant-abutment interface overdenture components and parametric evaluation of Equator® and Locator® prosthodontics attachments, Materials (Basel). 12 (2019). https://doi.org/10.3390/ma12040592.

[18] V. Filardi, Stress shielding FE analysis on the temporomandibular joint, J. Orthop. 18 (2020) 63–68. https://doi.org/10.1016/j.jor.2019.09.013.

[19] P. Marcián, J. Wolff, L. Horáčková, J. Kaiser, T. Zikmund, L. Borák, Micro finite element analysis of dental implants under different loading conditions, Comput. Biol. Med. 96 (2018) 157–165. https://doi.org/10.1016/j.compbiomed.2018.03.012.

[20] G. Cervino, U. Romeo, F. Lauritano, E. Bramanti, L. Fiorillo, C. D'Amico, D. Milone, L. Laino, F. Campolongo, S. Rapisarda, M. Cicciù, Fem and Von Mises Analysis of OSSTEM ® Dental Implant Structural Components: Evaluation of Different Direction Dynamic Loads, Open Dent. J. 12 (2018) 219–229. https://doi.org/10.2174/1874210601812010219.

[21] F. Mangano, L. Chambrone, R. Van Noort, C. Miller, P. Hatton, C. Mangano, Direct metal laser sintering titanium dental implants: A review of the current literature, Int. J. Biomater. 2014 (2014). https://doi.org/10.1155/2014/461534.

[22] S. Restrepo Klinge, No TitleEΛΕΝΗ, Αγαη. 8 (2019) 55.

[23] J. W. Nicholson, Titanium Alloys for Dental Implants: A Review, Prosthesis. 2 (2020) 100–116. https://doi.org/10.3390/prosthesis2020011.

[24] M.V. dos Santos, C.N. Elias, J.H. Cavalcanti Lima, The effects of superficial roughness and design on the primary stability of dental implants, Clin. Implant Dent. Relat. Res. 13 (2011) 215–223. https://doi.org/10.1111/j.1708-8208.2009.00202.x.